Human Molecular Genetics, 2004, Vol. 13, No. 18 **2133–2141**
doi:10.1093/hmg/ddh219
Advance Access published on July 21, 2004

Dysfunction of axonemal dynein heavy chain Mdnah5 inhibits ependymal flow and reveals a novel mechanism for *hydrocephalus* formation

Inés Ibañez-Tallon[1], Axel Pagenstecher[2], Manfred Fliegauf[3], Heike Olbrich[3], Andreas Kispert[4], Uwe-Peter Ketelsen[3], Alison North[5], Nathaniel Heintz[1] and Heymut Omran[3,*]

[1]Laboratory of Molecular Biology, Howard Hughes Medical Institute, Rockefeller University, New York, 10021 NY, USA, [2]Department of Neuropathology, Albert-Ludwigs-University, 79106 Freiburg, Germany, [3]Department of Pediatric Neurology and Muscle Disorders, Albert-Ludwigs-University, 79106 Freiburg, Germany, [4]Institut für Molekularbiologie, Medizinische Hochschule Hannover, 30625 Hannover, Germany and [5]Bio-Imaging Resource Center, Rockefeller University, 1230 York Avenue, New York, NY 10021, USA

Received June 1, 2004; Revised and Accepted July 9, 2004

Motility of unicellular organisms occurred early in evolution with the emergence of cilia and flagella. In vertebrates, motile cilia are required for numerous functions such as clearance of the airways and determination of left–right body asymmetry. Ependymal cells lining the brain ventricles also carry motile cilia, but their biological function has remained obscure. Here, we show that ependymal cilia generate a laminar flow of cerebrospinal fluid through the cerebral aqueduct, which we term as 'ependymal flow'. The axonemal dynein heavy chain gene *Mdnah5* is specifically expressed in ependymal cells, and is essential for ultrastructural and functional integrity of ependymal cilia. In *Mdnah5*-mutant mice, lack of ependymal flow causes closure of the aqueduct and subsequent formation of triventricular *hydrocephalus* during early postnatal brain development. The higher incidence of aqueduct stenosis and *hydrocephalus* formation in patients with ciliary defects proves the relevance of this novel mechanism in humans.

INTRODUCTION

Cilia are hair-like organelles extending from the cell membrane with either motile or sensory functions. In the unicellular alga *Chlamydomonas rheinhardtii* and in sperm, flagella resembling motile cilia, propel cells through a fluid. In vertebrates, multiple motile cilia or motile monocilia are located on various epithelial cells and move extracellular fluid. These include the respiratory epithelium of the airways, the embryonic node and the ependyma of the brain ventricles (1). Axonemal dyneins are the molecular motors that generate the movement of motile cilia and flagella by ATPase dependent reactions. Dynein heavy chain proteins assemble with intermediate and light chains into multiprotein complexes to form outer and inner dynein arms (ODA and IDA, respectively) which are attached to the axonemal microtubules (2). The very large dynein heavy chains form the globular heads and the stem of the complexes, and contain the ATPase and microtubule motor domains (3).

The ODA of the biflagellate alga *Chlamydomonas* comprises three (α-, β- and γ-) heavy chains. Mutations of the γ-heavy chain gene result in slow-swimming algae with ultrastructural axonemal defects in the ODA (4). The human and murine orthologs of *Chlamydomonas* γ-heavy chain are *DNAH5* and *Mdnah5*, respectively. Recessive mutations of *DNAH5* and *Mdnah5* cause primary ciliary dyskinesia (PCD) (5,6). Symptoms of PCD include chronic respiratory infections and randomization of *body situs* (7). Respiratory cilia in affected patients and in mutant mice are immotile and completely lack ODAs. As a result of cilia immotility, affected individuals show impaired mucociliary clearance, which accounts for the observed chronic respiratory infections. Similarly, dysfunction of cilia at the embryonic node most likely results in random left/right axis determination and *situs inversus* in half of the affected patients and mutant mice (5,6). Consistently, *Mdnah5* is specifically expressed in the respiratory epithelium and in the ventral surface of the node (5,8). In addition, *Mdnah5*-deficient mice develop severe *hydrocephalus* at early postnatal ages (6).

*To whom correspondence should be addressed. Tel: +49 7612704301; Fax: +49 7612704344; Email: omran@kikli.ukl.uni-freiburg.de

Mutant mice with deficiencies in other axonemal proteins (Spag6) or in components involved in ciliogenesis (polaris, polymerase λ and Hfh-4) have also been reported to develop *hydrocephalus* (9–12). Moreover, WIC-Hyd rats and SUMS/NP mice are common hydrocephalic animal models with cilia-related but as yet unidentified genetic defects (13,14). These findings clearly indicate a link between *hydrocephalus* formation and cilia dysfunction. Interestingly, *hydrocephalus* has also been reported in patients with PCD, which suggests that cilia dysfunction might also contribute to human *hydrocephalus* formation (15–21). However, the precise mechanism that links cilia dysfunction to *hydrocephalus* formation has not been elucidated so far. Therefore, we investigated the role of axonemal dynein heavy chain Mdnah5 in ependymal cilia function and cerebrospinal fluid flow. We show that *Mdnah5* is specifically expressed in ependymal cells lining the brain ventricles and the aqueduct. Mdnah5 deficiency results in cell-specific ultrastructural ODA defects in ependymal cilia. We demonstrate that ependymal cilia motility produces a directional 'ependymal flow' of the cerebrospinal fluid through the brain ventricles and the aqueduct. Furthermore, the absence of this ependymal flow is associated with the closure of the cerebral aqueduct during early postnatal brain development in *Mdnah5*-deficient mice, which subsequently leads to the formation of *hydrocephalus*. Thus, we show for the first time that a direct functional connection exists between the laminar flow produced by ependymal cilia and the correct development of the ventricular system during early postnatal brain development.

RESULTS

Mdnah5 is expressed in ciliated ependymal cells lining the brain ventricles

Axonemal dynein heavy chains are highly conserved in evolution, and have retained their role as molecular motors of motile cilia and flagella (22). We have previously shown that *Mdnah5* is expressed in motile respiratory cilia. We assumed that Mdnah5 is also an axonemal component of motile ependymal cilia. To confirm this, we carried out *in situ* hybridization experiments on brain sections from adult wild-type mice (Fig. 1). *Mdnah5* is specifically expressed in ependymal cells lining the brain ventricles and the aqueduct. Expression of *Mdnah5* was not seen in other cell types of the brain, which indicates an exclusive role in ciliated ependymal cells.

Partial deficiency of ODA in ependymal cilia of *Mdnah5*-deficient mice

Mutations in the orthologous dynein heavy chain genes *γ-HC, DNAH5* and *Mdnah5* have been shown to cause a loss of ODA in axonemes from *Chlamydomonas* and respiratory cilia from humans and mice, respectively. To test whether deficiency of *Mdnah5* also affects the ultrastructure of ependymal cilia, we performed transmission electron microscopy on brain samples from *Mdnah5*-deficient mice and control littermates (Fig. 2). To circumvent that secondary changes caused by increased intraventricular pressure lead to artificial results, we exclusively examined cilia derived from the fourth ventricle (Fig. 4). In both *Mdnah5*-deficient mice, we found a variable degree of ODA deficiency ranging from 0 to 5 ODA per cilium. This observation was supported by a large number of examined cilia. To calculate the mean number of ODA per cilium, we used only transverse sections (originating from both animals), which show all doublets in high quality. An average of 2.3 ODA ($n = 29$) per transverse section was found in *Mdnah5*-deficient mice in contrast to eight in wild-type mice. Thus, the number of ODA in ependymal cilia of *Mdnah5*-deficient mice is markedly reduced.

Ependymal cilia produce a directed fluid flow, which is absent in *Mdnah5*-deficient mice

We next assessed, whether the observed ultrastructural alterations affect the motility of the ependymal cilia. We carried out high-speed video recordings using differential interference contrast (DIC) and fluorescence microscopy on brain samples in the presence of a liquid suspension of fluorescent latex beads. In wild-type mice brains (Fig. 3A), the fast and synchronized movement of ependymal cilia produced a laminar fluid flow above the surface of the ependymal cells. The fluid flow caused a continuous movement of fluorescent beads (Supplementary Material). This result indicates that the ependymal cilia lining the brain ventricles produce a constant directed flow of cerebrospinal fluid. We term this movement as 'ependymal flow' in analogy to the 'nodal flow' of the extraembryonic perinodal fluid generated by nodal cilia.

In contrast, the beat frequency of ependymal cilia from *Mdnah5*-deficient mice was severely reduced, irregular and unsynchronized compared with control littermates (Supplementary Material), and therefore unable to move fluorescent beads in a continuous and directed manner (Fig. 3B). Movement of fluorescent beads was random and indistinguishable from background movement (Fig. 3C). We concluded, that the ependymal flow is absent in *Mdnah5*-deficient mice because of the dysmotility of ependymal cilia in these animals.

Mdnah5-deficient mice develop *hydrocephalus* owing to closure of the cerebral aqueduct

Our ultrastructural and functional data showed that cilia motility and ependymal flow are severely impaired in *Mdnah5*-mutant mice. As previously reported (6), *hydrocephalus* occurs in all mice homozygous for *Mdnah5* insertional mutation and becomes pathologically evident by enlarged head sizes at early postnatal age. The condition is progressive and affected mice grow to markedly smaller size than wild-type littermates and die before breeding age. To determine how the absence of ependymal flow affects the development of the ventricular system and when the *hydrocephalus* forms, we examined the brain morphology of *Mdnah5*-mutant mice and control littermates at different embryonic and early postnatal ages in serial sagittal and coronal semi-thin sections. At embryonic day 16.5 (E16.5) ($n = 2$), postnatal day 0.5 (P0.5) ($n = 2$) and P2 ($n = 2$) brains from *Mdnah5*-deficient mice were indistinguishable from controls and did not show any indication of *hydrocephalus* or aqueduct aberrations

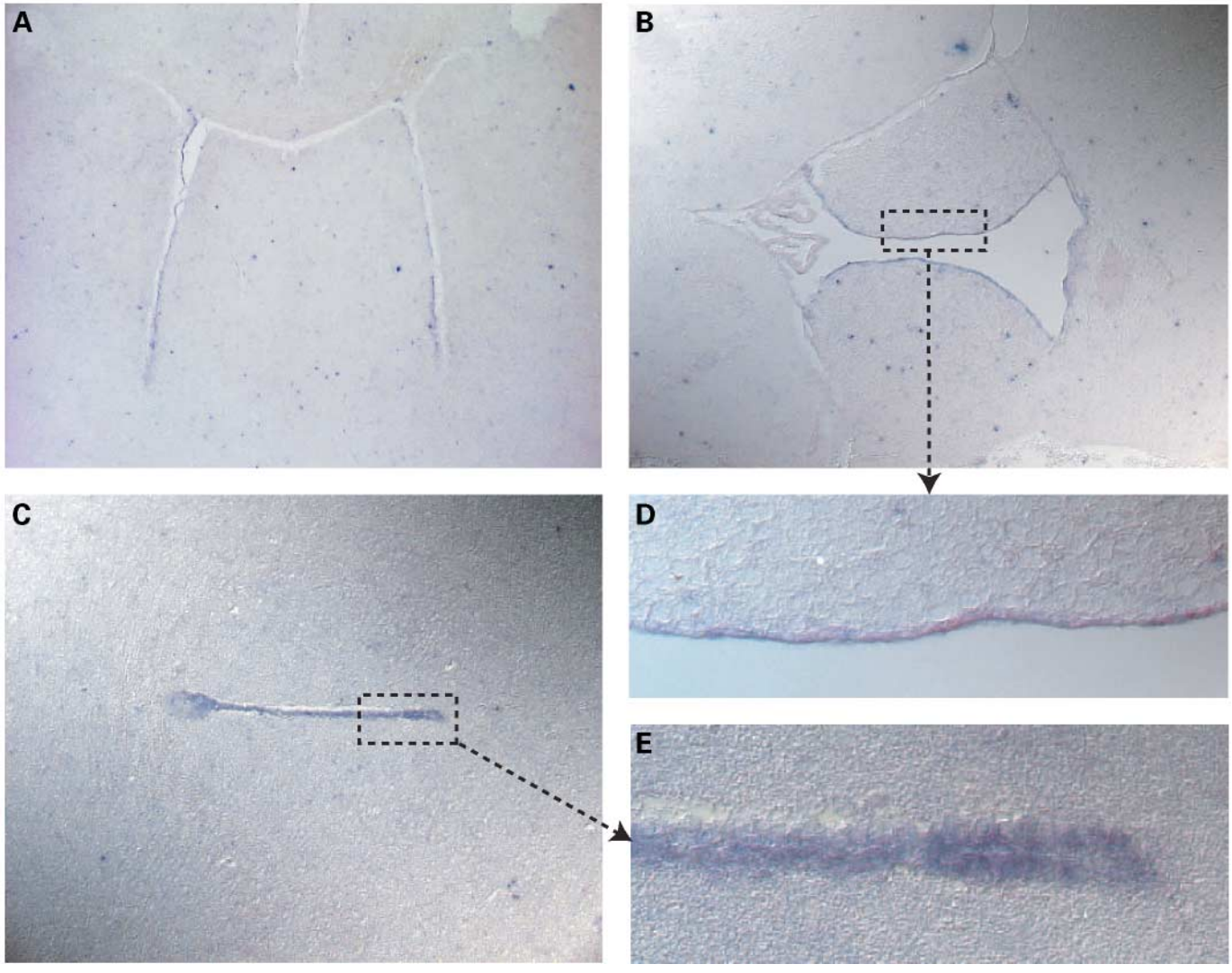

Figure 1. *Mdnah5* expression is restricted to ependymal cells. Section *in situ* hybridization analysis of *Mdnah5* expression in adult wild-type mice brains show specific staining in (**A**) lateral ventricles, (**B**) in the third ventricle and (**C**) the aqueduct of Sylvius. (**D**, **E**) Higher magnifications of details from (B) and (C), respectively. Please note the cilia on the ependymal cell surface.

(Fig. 4A and B). These findings demonstrate that *Mdnah5* deficiency does not cause congenital brain malformation. However, in *Mdnah5*-deficient mice brains ($n = 12$) at early postnatal ages (days 6, 12 and 19) we noticed formation of triventricular *hydrocephalus* with massive dilatation of the lateral ventricles and enlargement of the third ventricle (Fig. 4C and D). Further observations include thinning of the cortex and compression and distortion of the diencephalon and striatum. The fourth ventricle was never enlarged, consistent with an obstruction of the cerebrospinal fluid flow at the site of the cerebral aqueduct (aqueduct of Sylvius). We observed obstructions of the ventricular system at different sites along the aqueduct in all hydrocephalic *Mdnah5*-deficient mice studied. Some animals displayed discontinuity of the central part of the aqueduct (Fig. 4E–G). Others showed aqueductal stenosis or abnormal stenotic narrowing of the third ventricle at the junction of the aqueduct.

Development of transient dilatation of brain ventricles or triventricular *hydrocephalus* in PCD patients

The specific finding of triventricular *hydrocephalus* formation due to aqueduct closure in *Mdnah5*-deficient mice prompted us to review medical records of PCD patients with DNAH5 mutations (5). Although *hydrocephalus* was not documented, a transient dilatation of lateral brain ventricles in the neonatal period was reported in one patient (F753). We also reviewed all available clinical data from 80 patients participating in a German genetic PCD study. Two of these PCD patients had a triventricular *hydrocephalus* with closure of the aqueduct, which is referred to as 'aqueduct stenosis' by clinical neurologists. In both patients, raised intraventricular pressure had to be relieved by neurosurgical therapy. The incidence of congenital hydrocephalus is usually estimated to be three per 1000 (23). However, aqueduct stenosis is only responsible for a

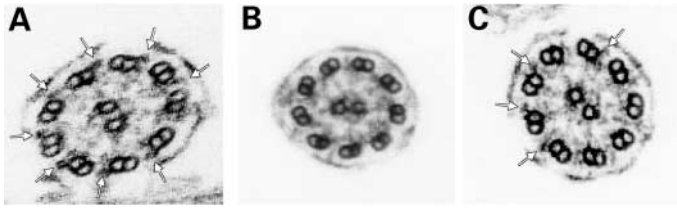

Figure 2. Transverse sections of ependymal cilia from *Mdnah5*-deficient mice show variable ODA defects. Transmission electron microscopy of ependymal cilia of the fourth brain ventricle show that (**A**) eight ODAs (arrows) are visible in the control, whereas different transverse sections of ependymal cilia from the same *Mdnah5*-deficient mouse show (**B**) total and (**C**) partial absence of ODAs. Arrows indicate the location of the remaining ODAs.

small proportion of congenital *hydrocephalus* cases. Incidence of aqueduct stenosis ranges from 2 to 16% (24,25). Therefore, a careful estimate for the incidence of congenital *hydrocephalus* caused by aqueduct stenosis is 3 per 10 000. Thus, the incidence of *hydrocephalus* caused by aqueduct stenosis in PCD patients (1 : 40) is significantly increased when compared with the general incidence of this disorder (3 : 10 000).

DISCUSSION

A role for ependymal cilia dysfunction in the etiology of *hydrocephalus* has been suggested on the basis of the occurrence of *hydrocephalus* in animal models with cilia defects (9–14). Likewise, humans affected by PCD are prone to a higher incidence of *hydrocephalus*. However, the specific mechanism linking cilia dysfunction with the development of *hydrocephalus* has remained unclear. Here, we report that axonemal dynein *Mdnah5*-mutant mice have dysfunctional ependymal cilia, ultrastructural ODA deficiencies and altered motility. Our studies demonstrate that normal ependymal cilia generate a directional flow of cerebrospinal fluid, which we term as 'ependymal flow'. This ependymal flow is absent in *Mdnah5*-deficient mice as a consequence of cilia dysmotility. Our anatomical examinations indicate that *Mdnah5* deficiency causes secondary closure of the aqueduct during early postnatal brain development and not congenital *hydrocephalus*, because anatomical alterations were first observed in early postnatal *Mdnah5*-deficient animals. Obstruction of the cerebrospinal fluid system at the site of the aqueduct explains the consecutive widening of the three proximal brain ventricles and the development of triventricular *hydrocephalus* in *Mdnah5*-deficient animals. We observed that closure of the aqueduct occurred, when the cerebral aqueduct lies within a very constricted flexure at the pontine level and becomes the narrowest and longest part for the passage of cerebrospinal fluid connecting the third and the fourth ventricles. This invagination, constriction and elongation take place only during late embryonic–early postnatal brain development (Fig. 5). On the basis of our functional data, we conclude that a steady ependymal flow generated by motile ependymal cilia lining the brain ventricles and the aqueduct is essential to maintain the structural integrity of the cerebral aqueduct during that critical time of brain development. On the contrary, if ependymal flow within the aqueduct is insufficient, as in the case of *Mdnah5*-deficient mice, secondary aqueduct closure and consecutive widening of the three brain ventricles located proximally from the occlusion (triventricular *hydrocephalus*) develop. Thus, we provide the first evidence that cilia movement is required for the propulsion of cerebrospinal fluid to avoid stenosis of the cerebral aqueduct during early postnatal development. Our data are supported by observations in the spontaneous WIC-Hyd rat mutant, a well-characterized animal model for PCD with unknown genetic defect (26). Similar to the results presented here, impaired ependymal ciliary motility has been demonstrated in hydrocephalic WIC-Hyd rats (27). However, the exact mechanism of *hydrocephalus* formation in these rats remained unknown, because obstructive lesions responsible for the origin of the *hydrocephalus* were not identified. Therefore, the WIC-Hyd model has been considered to be a non-obstructive *hydrocephalus* model. In this report, serial sections of the aqueductal region enabled us to detect aqueduct closure in *Mdnah5*-deficient mice. In light of our results, animal models with cilia-related defects should be specifically investigated for the presence of aqueduct alterations. *Hydrocephalus* development in mutant mice with deficiencies in the axonemal protein Spag (at 6–8 weeks after birth) or in polymerase λ involved in ciliogenesis (soon after birth) is also compatible with a secondary aqueduct closure in these animal models (9,11).

The specific finding of triventricular *hydrocephalus* formation due to aqueduct stenosis in *Mdnah5*-deficient mice prompted us to study the relevance of this mechanism in humans. We did not find evidence for *hydrocephalus* formation in PCD patients carrying *DNAH5* mutations (5). However, we found triventricular *hydrocephalus* with aqueduct stenosis in two of 80 PCD patients, which clearly indicates a higher incidence of this rare disorder in PCD patients. This observation is in agreement with other case reports of *hydrocephalus* in PCD patients (15–21). We conclude that cilia dysmotility is not sufficient for *hydrocephalus* formation but increases the risk for *hydrocephalus* development in humans. The brain morphology of humans with a shorter and wider aqueduct compared with mice, most likely explains the reduced vulnerability for secondary aqueduct occlusion in PCD patients. Vice versa, human individuals with an in-born narrow aqueduct might only develop *hydrocephalus*, if an additional primary or secondary (i.e. caused by bacterial toxins in meningitis) ependymal cilia dysfunction is present. *Hydrocephalus* is a frequent neurological disorder commonly caused by obstruction or malabsorption of cerebrospinal fluid (23). We propose here a novel mechanism, termed ependymal flow, as a relevant factor contributing to obstructive triventricular *hydrocephalus* in human patients.

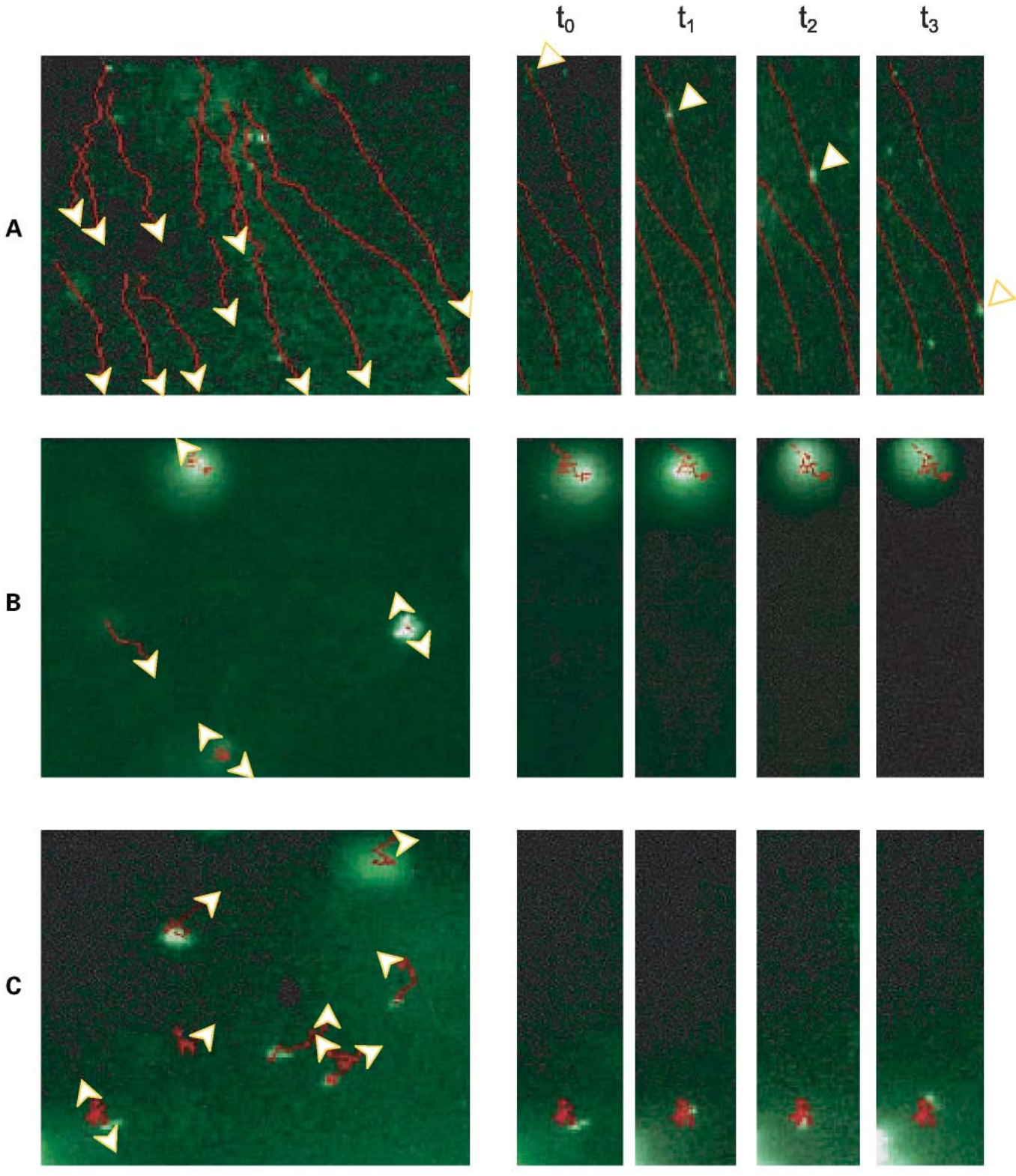

Figure 3. Ependymal flow produced by ciliary activity in wild-type mouse brain ventricles is absent in *Mdnah5*-deficient mice. (**A**) Movement of fluorescent particles visualizes the directed laminar 'ependymal flow' (red lines/arrows) in the wild-type control. Yellow arrows indicate a fluorescent particle along its trace (right panel). Particles move with an average flow velocity of 21.84 μm/s. (**B**) *Mdnah5*-deficient mice lack ependymal flow. The residual particle movements are indistinguishable from (**C**) background. A total of 200 frames were recorded over a period of 11.72 s (17 frames/s). Four individual images at different times; t_0, t_1: 0.77 s, t_2: 2.99 s and t_3: 6.98 s are shown on the right.

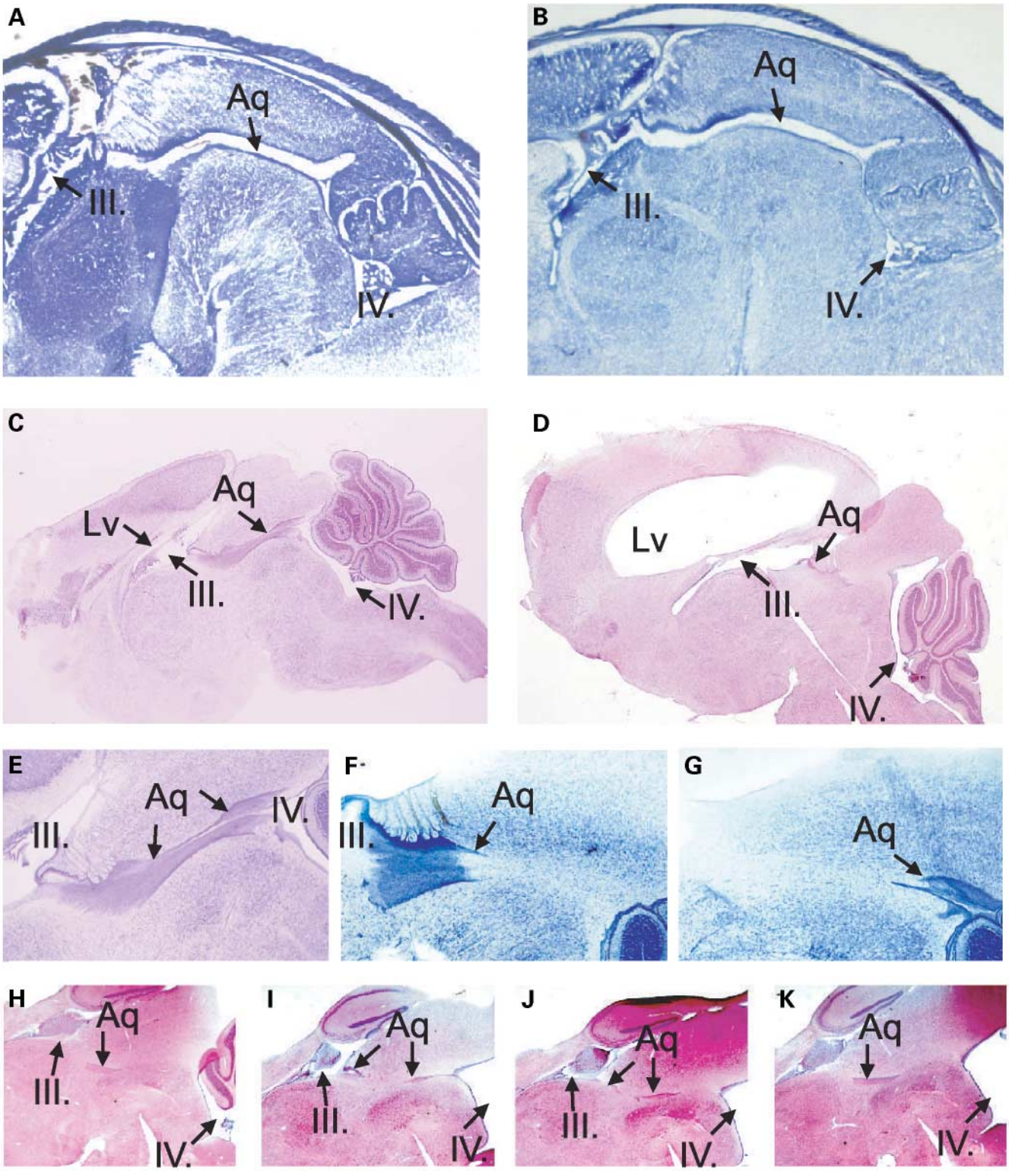

Figure 4. *Mdnah5*-deficient mice develop triventricular *hydrocephalus* owing to closure of the ventricular system at different sites along the cerebral aqueduct. (**A**, **B**) Sagittal brain sections of P0.5 control and *Mdnah5*-deficient mice show patent aqueducts connecting the third and fourth ventricles. (**C**) Normal brain anatomy of a control mouse (P12). (**D**) Hydrocephalic brain of an *Mdnah5*-deficient mouse (P12) with enlargement of both lateral ventricles and the third ventricle. The size of the fourth ventricle is normal. (**E**) Higher magnification of normal aqueduct anatomy (C). (**F** and **G**) Consecutive serial sagittal brain sections demonstrate aqueduct discontinuity in another *Mdnah5*-deficient mouse brain (P12). The proximal (F) and the distal part of the aqueduct (G) are closed and lack connection, because the central part of the aqueduct is missing. (**H**–**K**) Consecutive sagittal brain sections of an additional *Mdnah5*-deficient mouse also demonstrate aqueduct discontinuity and show abnormal narrowing of the aqueduct. III, IV, Lv, third, fourth, lateral ventricles; aq, respectively aqueduct.

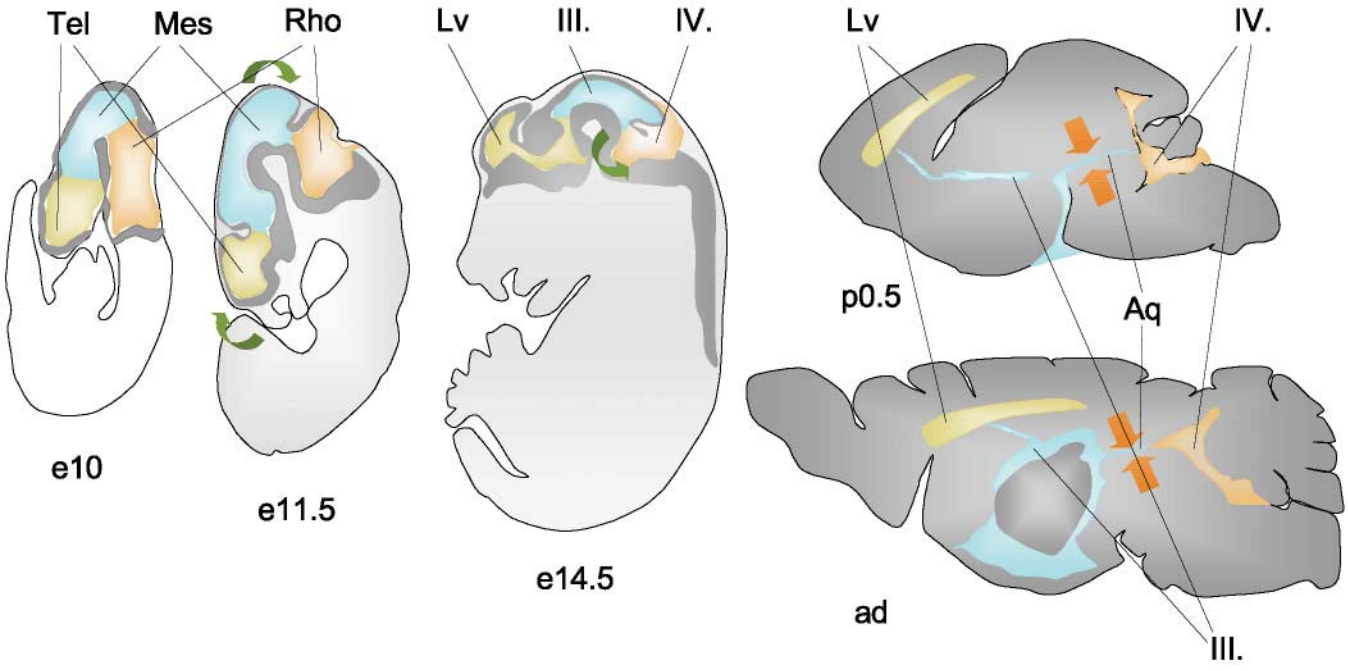

Figure 5. Representative scheme of the ventricular system during mouse brain development [E10, E11.5, E14.5, P0.5 and adult (Ad)]. At E10 the brain has developed from the anterior end of the neural tube into three primary vesicles: telencephalic (yellow), mesencephalic (blue) and rhombencephalic (orange). Later the lateral (I and II), third and fourth ventricles develop. Cerebrospinal fluid, predominantly produced in the lateral ventricles is transported through the ventricular system and enters the subarachnoid space through *foramina* at the fourth ventricle, where it is finally re-absorbed. During late embryonic brain development the cerebral aqueduct connecting the third and fourth ventricle is formed and becomes the narrowest part of the cerebrospinal fluid system.

So far, cell-specific differences between motile cilia of different origin are poorly understood. Variability in the beating pattern, movement frequency and length between respiratory and ependymal cilia have been observed (28). As in other motile cilia, respiratory and ependymal cilia have two central microtubules and nine peripheral microtubule doublets with dynein arms (1). Identical axonemal ultrastructures regarding the IDAs and the ODAs have been reported for both cilia types. In this report, we show that ependymal cilia in *Mdnah5*-deficient mice have partial absence of ODAs and severely reduced motility. Interestingly, we previously showed that the same mutation causes complete absence of ODAs and immotility in respiratory cilia (6). The observed differences provide novel evidence that the molecular composition of ciliary axonemes varies between cell-specific cilia types. Identification of the differences in the molecular architecture of respiratory and ependymal cilia will help to gain insight into the mechanisms that generate and control the cilia beat.

To avoid associated morbidity, prevention of *hydrocephalus* is an important goal of health care. Recent interventional studies in cultured rat brainstem slices have shown that application of serotonin can significantly increase the beat frequency of ependymal cilia (29). This observation suggests strategies to control cilia movement *in vivo* by administration of neurotransmitters and/or interference of signaling pathways. Our findings will aid the understanding of *hydrocephalus* formation and might help to identify new therapeutic options for the prevention or treatment of this common neurological disorder using ependymal cilia as a novel target.

MATERIALS AND METHODS

In situ hybridization experiments on brain sections from adult wild-type mice

In situ hybridization experiments on brain sections from adult wild-type mice using a 1.1 kb digoxigenin labeled antisense riboprobe transcribed from an *Mdnah5*-cDNA clone (AA880561) were performed as described following a published modification (30,31). Color reactions were extended up to 4 days to visualize the weak expression in the brain ventricles. Specimens were photographed using a Leica DC200 digital camera on a Leica M420 photomicroscope or under Nomarski optics using a Fujix digital camera HC300Z on a Zeiss Axioplan.

Ultrastructural analysis of ependymal cilia

Ultrastructural analyses of ependymal cilia were performed by transmission electron microscopy (Zeiss EM 900) on brain samples from two *Mdnah5*-deficient mice and two control littermates according to the standard procedures (32). We examined cilia of the fourth ventricle to circumvent artificial secondary changes caused by increased intraventricular pressure.

Videomicroscopic analysis of ependymal cilia function

Ependymal cilia function was analyzed by video microscopy using a Princeton Instruments Pentamax intensified CCD camera mounted on a Zeiss Axiovert 200 microscope with

a 100 × 1.3 NA objective and DIC imaging. Studies were performed on fresh brain samples obtained from nine *Mdnah5*-deficient animals and seven age-matched control littermates at ages ranging from P 7 to P 14. Immediately after euthanasia by decapitation, brains were removed from the skull and kept in sterile L-15 oocyte medium (specialty media) at room temperature. Under a dissecting microscope, brains were cut sagittally into two using a sharp blade, and tissue brushings of the brain ventricles were performed using a small brush with plastic bristles. Tissue brushing suspensions were collected in eppendorf tubes, kept in L-15 medium at room temperature and processed immediately. Before videomicroscopy analysis, 0.1 ml of tissue brushing suspensions, either alone or mixed with 10 μl of a 0.1% suspension of green fluorescent latex beads (0.046 μm, Sigma) were transferred to the central chamber of a 35 mm glass-bottom microwell dish for inverted microscopes (Plastek cultureware). For each mouse studied, the average processing time from euthanasia to videomicroscopy analysis was of 10 min. In each case the samples were examined at the microscope for 10–30 min at room temperature. During that time no change of flow characteristics was noted. We monitored the spontaneous particle movement of the fluorescent beads suspension as background control. For documentation of ependymal flow directionality and ciliary beating pattern 200 frames were recorded over a period of 7.14 s (28 frames/s). Recordings were analyzed by using MetaMorph software (Universal Imaging). A similar method was described for measurement of the nodal flow (33).

Brain pathology of *Mdnah5*-deficient and control mice

We determined the origin of *hydrocephalus* in *Mdnah5*-deficient and control mice in serial sagittal and coronal semi-thin sections. Brains of mice were analyzed at various ages ranging from E16.5 to P12. The sections were stained using routine protocols.

Incidence of *hydrocephalus* in PCD patients

Medical data available from PCD patients enrolled in a German genetic PCD study were evaluated for evidence of intrauterine dilatation of brain ventricles or *hydrocephalus* formation.

SUPPLEMENTARY MATERIAL

Supplementary Material is available at HMG online.

ACKNOWLEDGEMENTS

We would like to thank D. Elreda for assistance with cilia motility recordings, D. Morales for help with mouse embryonal studies and M. Petry for technical assistance. We are grateful for the help of the German patient support group 'Primaere Ciliaere Dyskinesie und Kartagener Syndrom e.V.' I.I.-T. and N.H. received support from the Howard Hughes Medical Institute. A.K., A.P. and H.O. were supported by the German Research Foundation (DFG Ki728/1, DFG Pa602/3 and DFG Om 6/2).

REFERENCES

1. Ibanez-Tallon, I., Heintz, N. and Omran, H. (2003) To beat or not to beat: roles of cilia in development and disease. *Hum. Mol. Genet.*, **12**, R27–R35.
2. El Zein, L., Omran, H. and Bouvagnet, P. (2003) Lateralization defects and ciliary dyskinesia: lessons from algae. *Trends Genet.*, **19**, 162–167.
3. King, S.M. (2000) The dynein microtubule motor. *Biochim. Biophys. Acta*, **1496**, 60–75.
4. Wilkerson, C.G., King, S.M. and Witman, G.B. (1994) Molecular analysis of the gamma heavy chain of Chlamydomonas flagellar outer-arm dynein. *J. Cell Sci.*, **107**, 497–506.
5. Olbrich, H., Haffner, K., Kispert, A., Volkel, A., Volz, A., Sasmaz, G., Reinhardt, R., Hennig, S., Lehrach, H., Konietzko, N. *et al.* (2002) Mutations in DNAH5 cause primary ciliary dyskinesia and randomization of left-right asymmetry. *Nat. Genet.*, **30**, 143–144.
6. Ibanez-Tallon, I., Gorokhova, S. and Heintz, N. (2002) Loss of function of axonemal dynein Mdnah5 causes primary ciliary dyskinesia and hydrocephalus. *Hum. Mol. Genet.*, **11**, 715–721.
7. Omran, H., Haffner, K., Volkel, A., Kuehr, J., Ketelsen, U.P., Ross, U.H., Konietzko, N., Wienker, T., Brandis, M. and Hildebrandt, F. (2000) Homozygosity mapping of a gene locus for primary ciliary dyskinesia on chromosome 5p and identification of the heavy dynein chain DNAH5 as a candidate gene. *Am. J. Respir. Cell Mol. Biol.*, **23**, 696–702.
8. Kispert, A., Petry, M., Olbrich, H., Volz, A., Ketelsen, U.P., Horvath, J., Melkaoui, R., Omran, H., Zariwala, M., Noone, P.G. and Knowles, M. (2003) Genotype–phenotype correlations in PCD patients carrying DNAH5 mutations. *Thorax*, **58**, 552–554.
9. Sapiro, R., Kostetskii, I., Olds-Clarke, P., Gerton, G.L., Radice, G.L. and Strauss, J.F., III (2002) Male infertility, impaired sperm motility, and hydrocephalus in mice deficient in sperm-associated antigen 6. *Mol. Cell. Biol.*, **22**, 6298–6305.
10. Taulman, P.D., Haycraft, C.J., Balkovetz, D.F. and Yoder, B.K. (2001) Polaris, a protein involved in left–right axis patterning, localizes to basal bodies and cilia. *Mol. Biol. Cell*, **12**, 589–599.
11. Kobayashi, Y., Watanabe, M., Okada, Y., Sawa, H., Takai, H., Nakanishi, M., Kawase, Y., Suzuki, H., Nagashima, K., Ikeda, K. and Motoyama, N. (2002) Hydrocephalus, situs inversus, chronic sinusitis, and male infertility in DNA polymerase lambda-deficient mice: possible implication for the pathogenesis of immotile cilia syndrome. *Mol. Cell. Biol.*, **22**, 2769–2776.
12. Chen, J., Knowles, H.J., Hebert, J.L. and Hackett, B.P. (1998) Mutation of the mouse hepatocyte nuclear factor/forkhead homologue 4 gene results in an absence of cilia and random left–right asymmetry. *J. Clin. Invest.*, **102**, 1077–1082.
13. Torikata, C., Kijimoto, C. and Koto, M. (1991) Ultrastructure of respiratory cilia of WIC-Hyd male rats. An animal model for human immotile cilia syndrome. *Am. J. Pathol.*, **138**, 341–347.
14. Bruni, J.E., Del Bigio, M.R., Cardoso, E.R. and Persaud, T.V. (1988) Neuropathology of congenital hydrocephalus in the SUMS/NP mouse. *Acta Neurochir.*, **92**, 118–122.
15. Rott, H.D. (1979) Kartagener's syndrome and the syndrome of immotile cilia. *Hum. Genet.*, **46**, 249–261.
16. Jabourian, Z., Lublin, F.D., Adler, A., Gonzales, C., Northrup, B. and Zwillenberg, D. (1986) Hydrocephalus in Kartagener's syndrome. *Ear Nose Throat J.*, **65**, 468–472.
17. de Santi, M.M., Magni, A., Valletta, E.A., Gardi, C. and Lungarella, G. (1990) Hydrocephalus, bronchiectasis, and ciliary aplasia. *Arch. Dis. Child*, **65**, 543–544.
18. Picco, P., Leveratto, L., Cama, A., Vigliarolo, M.A., Levato, G.L., Gattorno, M., Zammarchi, E. and Donati, M.A. (1993) Immotile cilia syndrome associated with hydrocephalus and precocious puberty: a case report. *Eur. J. Pediatr. Surg.*, **3** (Suppl. 1), 20–21.
19. Zammarchi, E., Calzolari, C., Pignotti, M.S., Pezzati, P., Lignana, E. and Cama, A. (1993) Unusual presentation of the immotile cilia syndrome in two children. *Acta Paediatr.*, **82**, 312–313.
20. al Shroof, M., Karnik, A.M., Karnik, A.A., Longshore, J., Sliman, N.A. and Khan, F.A. (2001) Ciliary dyskinesia associated with hydrocephalus and mental retardation in a Jordanian family. *Mayo Clin. Proc.*, **76**, 1219–1224.
21. Wessels, M.W., den Hollander, N.S. and Willems, P.J. (2003) Mild fetal cerebral ventriculomegaly as a prenatal sonographic marker for Kartagener syndrome. *Prenat. Diagn.*, **23**, 239–242.

22. Holzbaur, E.L. and Vallee, R.B. (1994) DYNEINS: molecular structure and cellular function. *Annu. Rev. Cell Biol.*, **10**, 339–372.
23. Aicardi, J. (1998) Hydrocephalus. In Aicardi, J. (ed.), *Diseases of the Nervous System*, 2nd edn. Mac Keith Press, London, UK, pp. 187–209.
24. Roume, J., Larroche, J.C., Razavi-Encha, F., Gonzales, M., Migne, G. and Mulliez, N. (1990) Fetal hydrocephalus. Clinical significance of associated anomalies and genetic counseling: a pathological approach. *Genet. Couns.* **1**, 185–196.
25. el Awad, M.E. (1992) Infantile hydrocephalus in the south-western region of Saudi Arabia. *Ann. Trop. Paediatr.* **12**, 335–338.
26. Koto, M., Miwa, M., Shimizu, A., Tsuji, K., Okamoto, M. and Adachi, J. (1987) Inherited hydrocephalus in Csk: Wistar-Imamichi rats; Hyd strain: a new disease model for hydrocephalus. *Jikken Dobutsu*, **36**, 157–162.
27. Nakamura, Y. and Sato, K. (1993) Role of disturbance of ependymal ciliary movement in development of hydrocephalus in rats. *Childs Nerv. Syst.*, **9**, 65–71.
28. O'Callaghan, C., Sikand, K. and Rutman, A. (1999) Respiratory and brain ependymal ciliary function. *Pediatr. Res.*, **46**, 704–707.
29. Nguyen, T., Chin, W.C., O'Brien, J.A., Verdugo, P. and Berger, A.J. (2001) Intracellular pathways regulating ciliary beating of rat brain ependymal cells. *J. Physiol.*, **531**, 131–140.
30. Parr, B.A., Shea, M.J., Vassileva, G. and McMahon, A.P. (1993) Mouse Wnt genes exhibit discrete domains of expression in the early embryonic CNS and limb buds. *Development*, **119**, 247–261.
31. Knecht, A.K., Good, P.J., Dawid, I.B. and Harland, R.M. (1995) Dorsal-ventral patterning and differentiation of noggin-induced neural tissue in the absence of mesoderm. *Development*, **121**, 1927–1935.
32. Walker, U.A., Bickel, M., Lutke Volksbeck, S.I., Ketelsen, U.P., Schofer, H., Setzer, B., Venhoff, N., Rickerts, V. and Staszewski, S. (2002) Evidence of nucleoside analogue reverse transcriptase inhibitor—associated genetic and structural defects of mitochondria in adipose tissue of HIV-infected patients. *J. Acquir. Immune. Defic. Syndr.*, **29**, 117–121.
33. Nonaka, S., Tanaka, Y., Okada, Y., Takeda, S., Harada, A., Kanai, Y., Kido, M. and Hirokawa, N. (1998) Randomization of left-right asymmetry due to loss of nodal cilia generating leftward flow of extraembryonic fluid in mice lacking KIF3B motor protein. *Cell*, **95**, 829–837.